Superlinear electron transport and noise in quantum wires

R. Mickevičius, V. Mitin, and U. K. Harithsa
Department of Electrical and Computer Engineering, Wayne State University, Detroit, Michigan 48202

D. Jovanovic and J. P. Leburton
Beckman Institute for Advanced Science and Technology and the Department of Electrical and Computer Engineering, University of Illinois, Urbana, Illinois 61801

(Received 21 June 1993; accepted for publication 14 October 1993)

We have employed a Monte Carlo technique for the simulation of electron transport and noise (diffusion) in GaAs rectangular quasi-one-dimensional quantum wire structures at low temperatures. It is demonstrated that with the heating of electron gas the efficiency of acoustic phonon scattering decreases and the mobility increases. The increase of electron mobility appears as a superlinear region on velocity-field dependence. It is shown that electron noise increases in the superlinear region. The transition from superlinear transport to the regime close to electron streaming with a further increase of electric fields is reflected on the diffusivity-frequency dependence by the appearance of a separate peak at the streaming frequency. The electron streaming regime which takes place at higher fields causes the collapse of the diffusion coefficient (noise spectral density) to the streaming frequency.

I. INTRODUCTION

Low-dimensional semiconductor structures and particularly quasi-one-dimensional (1D) structures of quantum wires (QWI) have recently attracted much attention due to the possibilities of achieving very high electron mobilities[1] and low-noise performance at low temperatures with possible technological applications. In spite of the fact that electric noise is a crucial device characteristic because it sets lower limits to the accuracy of any measurement, there are almost no studies on electron noise in QWIs at low temperatures. The reason is that electron transport and noise in quantum wires at low and intermediate temperatures, and at intermediate electric fields are primarily controlled by acoustic-phonon scattering. It is common practice to treat acoustic-phonon scattering within elastic or quasi-elastic approximations (see, e.g., Refs. 2–5) as in bulk materials. However, it has been shown earlier[6] that acoustic-phonon scattering in low-dimensional structures and particularly in QWIs is essentially inelastic and is far more important for electron energy and momentum relaxation than in bulk materials. Correct treatment of acoustic-phonon scattering in low-dimensional structures requires full consideration of uncertainty of momentum conservation (*quasi-conservation*).[6]

Due to peculiarities of acoustic-phonon scattering in QWIs, electron kinetic and noise parameters may be considerably different from those in bulk materials. This is due to the dependence of the 1D density of states on electron energy whereby the acoustic-phonon scattering rate decreases with an increase in electron energy, excluding the region close to the subband bottom.[6] As a result, the efficiency of electron scattering by acoustic phonons should decrease with the electron heating by electric fields. At rather low electric fields, where electrons are still below the optical-phonon energy, it is expected that the decrease in the efficiency of acoustic-phonon scattering might lead to an increase in electron mobility.[7] In real structures, however, acoustic-phonon scattering may be either too weak, resulting in an electron runaway towards the optical-phonon energy, or too strong so that electrons cannot be heated at all up to very high electric fields. It seems, however, that there should be optimum structure parameters for which an increase in electron mobility can be quite pronounced.

The aim of the present paper is to get an insight into electron transport and noise in rectangular QWIs at low temperatures for a wide range of electric fields through the study of velocity-field and energy-field characteristics as well as electron noise spectral density. We developed a Monte Carlo code which efficiently includes electron scattering by acoustic as well as by optical phonons and allows simulation of electron transport and noise in 1D structures.

II. MODEL AND METHOD

We consider rectangular GaAs QWIs with several different cross sections embedded into AlAs material. We assume that the electron gas is nondegenerate with electron concentration of the order of 10^5 cm^{-1} or less. Electron scattering by confined longitudinal optical (LO) phonons and localized surface (interface) optical (SO) phonons[8] as well as by bulklike acoustic phonons[6] has been taken into account. Ionized impurities are assumed to be located sufficiently far from the QWI so that their influence on the electron motion inside the wire is negligible. Our program incorporates all subbands occupied by electrons, but for the present structure parameters only the first two or three subbands are relevant to the electron transport at low temperatures. The transition probabilities are given by

$$W(k_x,k_x',\mathbf{q})=\frac{2\pi}{\hbar}\,|M(k_x,k_x',\mathbf{q})|^2 \times\delta[\epsilon(k_x')-\epsilon(k_x)-\Delta\epsilon\pm\hbar\omega_{\mathbf{q}}]\,. \quad (1)$$

 0021-8979/94/75(2)/973/6/$6.00

Here, $M(k_x,k_x',\mathbf{q})$ represents the matrix element for a transition from the initial k_x state to the final k_x' state mediated by a phonon with wave vector $\mathbf{q}$, and $\Delta\epsilon$ is the intersubband separation energy. The $\pm$ sign in the energy-conserving δ function accounts for the emission $(+)$ and absorption $(-)$ of phonons. The total scattering rate from an initial state with energy ϵ is then given by

$$\lambda(k_x)=\frac{V}{(2\pi)^3}\sum_{k_x'}\int d\mathbf{q}\, W(k_x,k_x',\mathbf{q})\,, \tag{2}$$

where the summation over the final k_x' states takes into account all the possible intrasubband and intersubband transitions.

The 1D electron scattering by LO and SO phonons is described in more detail in Ref. 8. Electron scattering by acoustic phonons is usually treated as an elastic mechanism, which is not true for low-dimensional structures. Let us take a closer look at electron interaction with acoustic phonons in a rectangular QWI. The acoustic-phonon scattering rate is given by[6]

$$\lambda(\epsilon)=\frac{E_a^2 k_B T}{4\pi^2\rho u^2\hbar^2}\sqrt{\frac{m^*}{2}}\int\frac{dq_y\,dq_z\,G(q_y,q_z)}{\sqrt{\epsilon\mp\hbar u q_T-\Delta\epsilon}}\,, \tag{3}$$

where E_a is the acoustic deformation potential, ρ is a material density, u is a sound velocity in the material, and $q_T=\sqrt{q_y^2+q_z^2}$ is a transverse component of the phonon wave vector. The function $G(q_y,q_z)$ is a form factor which represents the uncertainty of momentum conservation in low-dimensional structures. The above equation as obtained in Ref. 6 assumes that $q_x \ll q_T$ and $\hbar u q_T \ll k_B T$. If the phonon energy under the delta function is neglected[5] one gets the elastic approximation:

$$\lambda(\epsilon)=\frac{E_a^2 k_B T}{\rho u^2\hbar^2 L_y L_z}\sqrt{\frac{m^*}{2(\epsilon-\Delta\epsilon)}}(1+\tfrac{1}{2}\delta_{jj'})(1+\tfrac{1}{2}\delta_{ll'})\,, \tag{4}$$

where indices j and l denote the initial subband, j' and l' denote the final subband, and L_y and L_z are transverse dimensions of the QWI. One can see that the elastic approximation of Eq. (4) yields two unphysical divergencies of the scattering rate: (i) when the electron energy goes to zero after scattering and (ii) when spatial dimensions of a QWI approach zero. Both these divergencies disappear within the inelastic approach of Eq. (3).[6]

In order to demonstrate the differences between the elastic and inelastic models we have plotted the scattering rate versus electron energy for the two different models in Fig. 1. Note that within the elastic approximation the absorption and emission rates are equal. One can see the elastic approximation highly overestimates the scattering rate in the low-energy region.

Computationally, the main differences between 1D simulations and 2D and bulk models is that phase space reduction lifts some of the complexities associated with computation of angular scattering. For instance, due to the limited number of final scattering states, the total rates can be stored in the memory, thereby eliminating lengthy computations during free-flight loops and final state selection.[9]

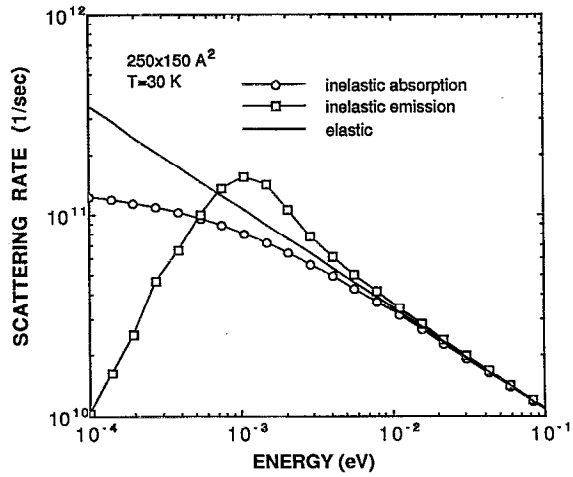

FIG. 1. Acoustic-phonon scattering rate vs electron energy for elastic and inelastic models of electron-phonon interaction. The emission and absorption rates are equal within the elastic approximation. The temperature and cross section are indicated on the figure.

We have developed a novel and very efficient procedure for random selection of acoustic-phonon energy involved in scattering. The essence of this procedure is that we first numerically perform a von Neumann procedure for a set of random numbers and tabulate the phonon energy as a function of a random number. Actually, we have solved the following equation:

$$r\int_{q_{T_{\min}}}^{q_{T_{\max}}} dq_T\,F(q_T)=\int_{q_{T_{\min}}}^{q_T^*} dq_T\,F(q_T)\,, \tag{5}$$

with respect to the unknown upper integration limit q_T^* for a set of 100 random values of r ranging from 0 to 1. Here the function $F(q_T)$ is an intergrand of Eq. (3) and represents the scattering probability dependence on the transverse components of the phonon wave vector. For a set of uniform random numbers $(r_1,r_2,\ldots,r_{100})$ we obtain the set of solutions of Eq. (5) $(q_{T_1}^*,q_{T_2}^*,\ldots,q_{T_{100}}^*)$ (which are transverse components of the phonon wave vector) distributed according to the probability $F(q_T)$ of electron scattering by the acoustic phonon with a given transverse component q_T. Since the transverse component of the phonon wave vector is directly related to the phonon energy within this approach,[10] one can find the desired phonon energy for each value of r. The tables of such values have been separately calculated for a set of electron energies for the emission and absorption of the acoustic phonon. Hence, the random choice of energy of the phonon involved in a scattering event in the Monte Carlo procedure is just the generation of the random number r and the selection of the corresponding phonon energy value from the appropriate table. This procedure essentially speeds up the Monte Carlo simulation.

As the transient process under near-streaming conditions lasts a very long time and electrons have to undergo a great number of scattering events before reaching the stationary regime, the conventional ensemble Monte Carlo simulation becomes essentially inefficient. We have devel-

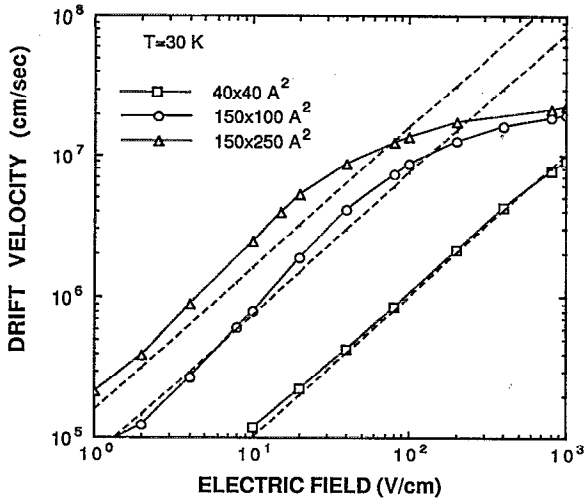

FIG. 2. Electron drift velocity as a function of applied electric field for three different cross sections of the quantum wire. Dashed lines show the drift velocity estimated from the low-field mobility. Wire cross sections and lattice temperatures are indicated on the figure.

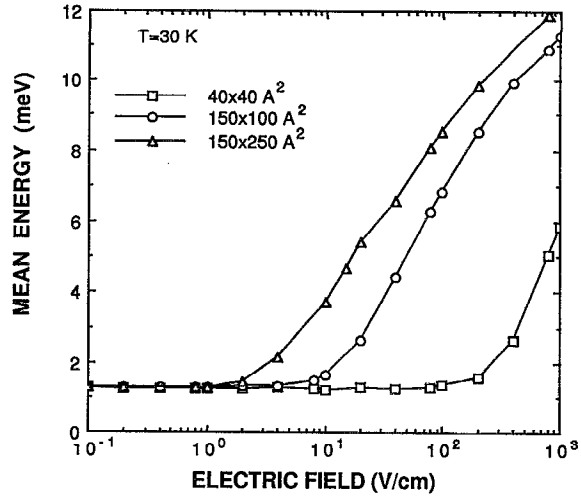

FIG. 3. Mean electron energy as a function of applied electric field for the same quantum wires as in Fig. 2.

oped an ensemble Monte Carlo technique[11] which permits a quick relaxation to steady state in the presence of long-lasting transient processes. The essence of this technique lies in the choice of the initial electronic state. We choose every next electron randomly from the trajectory of the previous electron so that we approach the stationary initial distribution function in three to four iterations. This technique has been used for velocity autocorrelation function calculations. All stationary characteristics have been calculated by the single-particle Monte Carlo technique, averaging over one electron trajectory.[12]

III. RESULTS AND DISCUSSION

The results presented here are obtained for $T=30$ K. Similar results have been obtained for temperatures $T=20$ and 77 K, and the characteristics are qualitatively the same as at 30 K.

Figure 2 shows the electron drift velocity as a function of applied electric field. For thick QWIs the superlinear region appears on the velocity-field dependence at an electric field of the order of 10 V/cm. With a decrease in the thickness of the QWI, the superlinear region shifts towards higher electric fields. The superlinear dependence disappears for the QWI with a cross section of 40×40 Å^2. As we have already pointed out in Sec. I, the superlinear dependence is a purely 1D effect caused by the reduction of the efficiency of acoustic-phonon scattering as the electron gas is heated. Figure 3 shows the mean electron energy plotted versus the electric field for the same QWIs. In 1D structures the thermal equilibrium electron energy corresponding to one degree of freedom is equal to $k_BT/2$, which at $T=30$ K is 1.3 meV. This equilibrium energy establishes well in our simulations, indicating that acoustic-phonon scattering is treated correctly. One can clearly see that electron heating starts at higher electric fields in thin QWIs. This is due to the fact that the rate of electron scattering by acoustic phonons increases when the thickness of a quantum wire decreases [within the elastic approximation (4) the rate of scattering is inversely proportional to the cross section of a QWI].

In thick QWIs electrons with the energy of the order of or higher than k_BT easily escape from acoustic-phonon scattering and run away up to the optical phonon emission threshold. A further increase in electric field leads to a near saturation of the drift velocity at a streaming value $v_s=\sqrt{\hbar\omega/m^*}=2.2\times10^7$ cm/s, where $\hbar\omega$ is the LO phonon energy.[11] This behavior is related to the electron transition from the superlinear to streaming regime. Under streaming conditions, acoustic-phonon scattering can no longer hold back low-energy electrons from reaching the optical-phonon scattering threshold to emit a phonon, in which case the electrons travel to the subband bottom, repeating this process again and again.[13] In the case of ideal streaming (infinitely high electron-optical phonon scattering rate and the absence of any other scattering mechanism) electrons oscillate in $\mathbf{k}$ space for an indefinite period of time, which leads to permanent oscillations of the electron drift velocity and mean energy.[14] In real conditions both the penetration through the optical-phonon scattering threshold and the acoustic-phonon scattering randomizes the phase of the electron ensemble, and even though each electron under certain conditions continues oscillating, the mean parameters approach stationary values. This problem has been investigated in Refs. 2 and 14.

To examine the superlinear region in more detail we have calculated the electron diffusion coefficient as a function of electric field in Fig. 4. The superlinear region is reflected on diffusivity-field dependence as a broad maximum. The maximum on the diffusivity curve is well pronounced for thick QWIs and almost disappears for a 40×40 Å^2 QWI. Electron scattering by acoustic phonons in this thin QWI is so strong that it prevents electron heating by the electric field up to very high values where optical phonon emission starts to dominate and electrons enter the

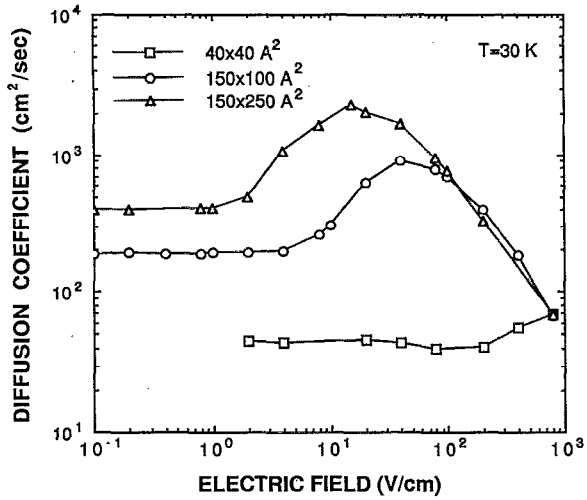

FIG. 4. Electron diffusion coefficient as a function of electric field for the same quantum wires as in Fig. 2.

streaming regime. The decrease in diffusivity at higher electric fields indicates the transition from superlinear electron transport to electron streaming.

The dependence of electron mobility on electric field can be easily extracted from velocity-field dependence (Fig. 2). We have estimated the low-field electron mobility for three different QWIs. The low-field mobility values of 1.5×10^4, 7×10^4, and 1.5×10^5 cm^2/V s are obtained for QWI cross sections of 40×40, 150×100, and 150×250 Å^2, respectively. Almost the same mobility values are derived from Einstein's relationship $\mu=eD/k_BT$, where D is the low-field diffusion coefficient (Fig. 4).

Figure 5 shows the electron distribution functions at different electric fields for a 250×150 Å^2 QWI. One can see that the distribution function in the intermediate energy region is flattened and extended up to the optical phonon energy. There is no electron penetration beyond

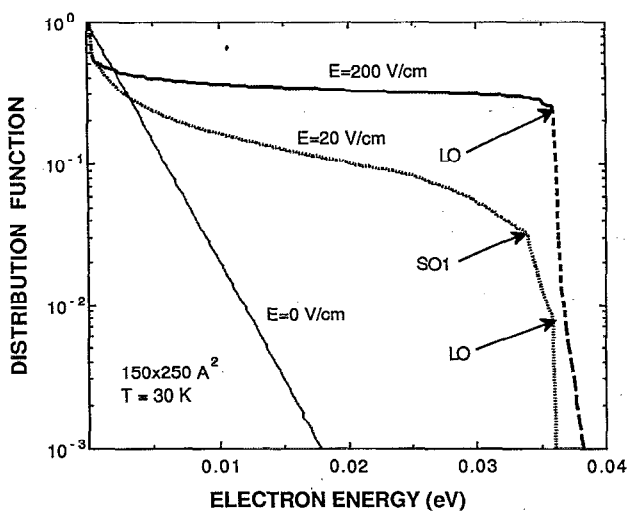

FIG. 5. Electron distribution function vs electron energy for three different electric fields. The quantum wire cross section is 150×250 Å.

the optical-phonon energy in the given fields, so that the distribution function is cut off at the phonon energy. At lower electric fields the cutoff energy in the electron distribution coincides with the lowest SO phonon energy, which is equal to 34.5 meV. At higher electric fields a fraction of the electrons penetrate beyond the SO phonon energy. However, the electron penetration beyond the LO phonon energy is very weak. The point is that electron scattering by LO phonons in this thick QWI is much stronger than electron scattering by SO phonons.[8] The distribution function at 20 and 200 V/cm has a steep slope at low energies, which can be characterized by a very low temperature (lower than the equilibrium temperature). There are not enough electrons accumulated at the subband bottom to assure the electron cooling effect. It has been shown in Ref. 11 that a simplified treatment of acoustic-phonon scattering leads to the cooling effect due to stronger scattering at the low-energy region and thus to the excess accumulation of electrons at the subband bottom after they have emitted optical phonons.

In the near-streaming regime, electrons have "a long memory" since their trajectory is periodically repeated. A powerful technique to recover this memory and to reveal the transition from a diffusive to a streaming regime is the analysis of the current density autocorrelation function.[14] Here we deal with a conservative electron ensemble with a spatially uniform electron concentration. Therefore, fluctuations of current density arise merely from the fluctuations of electron velocity. That is the reason why, instead of analyzing the current density autocorrelation function, we prefer to consider the velocity autocorrelation function given by

$$C(T)=\langle \delta v(t)\delta v(t+T)\rangle , \tag{6}$$

where the angular brackets stand for an average over time t, and $\delta v(t)=v(t)-v_d$ is the deviation from the drift velocity v_d at time t. The dependence of autocorrelation function on delay time T contains information on all characteristic times of the given conservative electron system.

Figure 6 shows autocorrelation functions plotted versus the delay time and calculated for different electric fields corresponding to the ohmic electron transport (zero electric field), the superlinear electron transport regime (20 V/cm), and the near-streaming regime (200 V/cm). The characteristic decay time increases as the electric field increases from 0 to 20 V/cm, reflecting the decrease in acoustic-phonon scattering efficiency responsible for a mobility increase at those fields. The negative autocorrelator which appears at 20 V/cm turns to damping oscillations when electrons approach the streaming regime (200 V/cm). The oscillation period coincides with the period of electron motion in k space:

$$t_s=\sqrt{2\hbar\omega m^*}/eE+\tau_{\rm op}, \tag{7}$$

where $\tau_{\rm op}$ is the effective optical-phonon emission time above optical-phonon energy. The characteristic oscillation decay time is mainly defined by the acoustic-phonon scattering rate since electron penetration into the active region where they can emit optical phonons is negligible at those

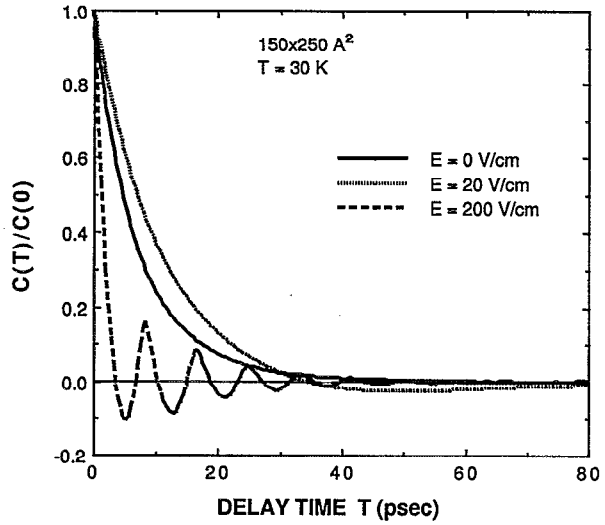

FIG. 6. Electron velocity autocorrelation function vs delay time at different electric fields for the same quantum wire as in Fig. 5.

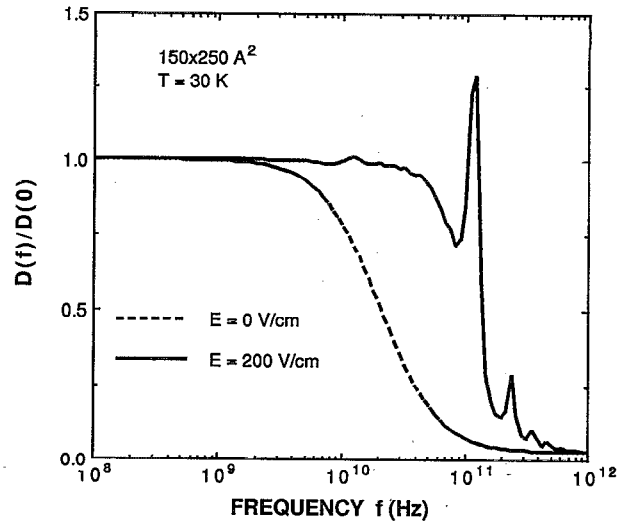

FIG. 7. Electron diffusion coefficient as a function of frequency at various electric fields for the same quantum wire as in Fig. 5.

electric fields. With a further increase of the electric field the efficiency of the acoustic-phonon scattering rate decreases (since electrons spend less and less time in the low-energy region) while their penetration into the active regions gets deeper. Therefore, at sufficiently high electric fields, electron streaming is controlled by penetration through the LO phonon emission threshold rather than by acoustic-phonon scattering. At very low electric fields, in the absence of acoustic-phonon scattering, electron streaming is controlled by the lowest-energy SO phonons. Even in this idealized case the streaming oscillations are slightly damped due to the electron penetration beyond the SO phonon energy.

The calculated autocorrelation functions have been used to calculate the frequency dependencies of the electron diffusion coefficient (velocity noise spectral density) related with the autocorrelation function through the Wiener–Khintchine theorem:

$$D(\omega)=\int_0^\infty dT\, e^{-i\omega T}C(T)\,. \tag{8}$$

The results are presented in Fig. 7. On the vertical scale we plotted the normalized diffusion coefficient, which in fact is merely the normalized noise power spectral density of the conservative electron system. The relationship between the spectral density and diffusion coefficient is given by[15]

$$S(\omega)=4D(\omega)\,. \tag{9}$$

The frequency dependence of the diffusion coefficient at zero field has a Lorentzian shape $(1+\omega^2\tau^2)^{-1}$, where τ is effective scattering time. (Practically the same Lorentzian dependence is obtained for 20 V/cm, i.e., at the maximum of diffusivity). The critical frequency $\omega_c=\tau^{-1}$ increases effectively with the onset of optical-phonon scattering. The effective time of electron scattering by optical phonons is determined primarily by the electric field, i.e., it is equal to the streaming time, [the first term of the time given by Eq. (7)], because electron penetration into the active region is still negligible [the second term in Eq. (7) may be neglected]. At higher electric fields when electron streaming takes through the electron diffusive motion, the peak related to the streaming frequency $f_s=1/t_s$ separates from the Lorentzian diffusivity-frequency dependence (see Fig. 7). Additional peaks also appear on frequencies that are multiples of the streaming frequency. The appearance of these peaks indicates the transition to the streaming regime. Note that critical Lorentzian frequency ω_c increases as electrons enter the streaming regime. With a further increase in electric field, the peak related to the streaming increases while the plateau of constant diffusivity is going down. The simulation of this regime in the presence of two very different characteristic times (streaming period is much less than the acoustic-phonon scattering time) is very complicated and does not provide good accuracy. In order to study pure streaming we have calculated the diffusivity-frequency dependence, ignoring acoustic-phonon scattering. In that case almost all diffusivity (noise) collapses to the streaming frequency and frequencies which are multiples of the streaming frequency.

IV. CONCLUSIONS

We have simulated the electron transport and noise (diffusivity) in rectangular GaAs/AlAs quantum wires at low and intermediate electric fields for $T=30$ K by the Monte Carlo technique. Due to heating of the electron system, the efficiency of electron scattering by acoustic phonons decreases and the mobility increases. The decrease of acoustic-phonon scattering efficiency is reflected by the velocity autocorrelation function, which has a longer decay time in that electric-field region. The increase in mobility is also reflected by the velocity-field dependence as a superlinear region. The appearance of enhanced mobility and the corresponding range of electric fields strongly depend on the thickness of a QWI. The point is

that the rate of electron scattering by acoustic phonons increases with a decrease in the cross section of a QWI. With a further increase in electric field, acoustic-phonon scattering can no longer hold back electrons from being heated by electric fields. As a result, electrons start to run away even from the subband bottom and the streaming regime is realized. The transition from diffusive electron transport regime to streaming has been studied by analyzing the frequency dependencies of the diffusion coefficient (noise spectral density). It is demonstrated that this transition is reflected on the latter dependence by the appearance of a separate peak at the streaming frequency. The electron thermal noise almost completely collapses to the streaming frequency and its higher harmonics in the pure streaming regime. Similar results have been obtained for temperatures of 20 and 77 K.

ACKNOWLEDGMENTS

The work of R. Mickevičius, V. Mitin, and U. K. Harithsa is supported by the National Science Foundation under Grant No. ECD 92-46559 and by Army Research Office under Grant 29541EL, and the work of D. Jovanovic and J. P. Leburton has been supported by Joint Services Electronics Program under Grant No. N00014-90-J-1270.

[1] H. Sakaki, Jpn. J. Appl. Phys. **19**, L735 (1980).
[2] D. Jovanovic and J. P. Leburton, Superlattices and Microstructures **11**, 141 (1992).
[3] B. K. Ridley, J. Phys. C. **15**, 5899 (1982).
[4] B. K. Ridley, Rep. Prog. Phys. **54**, 169 (1991).
[5] F. Comas, C. Trallero Giner, and J. Tutor, Phys. Status Solidi B **139**, 433 (1987).
[6] V. Mitin, R. Mickevičius, and N. Bannov, Proceedings of the International Workshop on Computational Electronics, Leeds, 1993, pp. 219–233 (unpublished).
[7] S. D. Beneslavski and V. A. Korobov, Sov. Phys. Semicond. **20**, 650 (1986).
[8] R. Mickevičius, V. Mitin, K. W. Kim, M. A. Stroscio, and G. J. Iafrate, J. Phys. Condens. Matter **4**, 4959 (1992).
[9] D. Jovanovic and J. P. Leburton, in *Monte Carlo Device Simulation: Full Band and Beyond*, edited by K. Hess (Kluwer, Dordrecht, 1991), p. 191.
[10] Within a more elaborate approach where the q_x components are not neglected, the phonon energy is uniquely related to q_x, so that one can use this relationship to generate a phonon energy for each value of r.
[11] R. Mickevicius, V. Mitin, D. Jovanovic, and J. P. Leburton, in Proceedings of the International Workshop on Computational Electronics, Urbana, Il, 1992, p. 293 (unpublished).
[12] C. Jacoboni and L. Reggiani, Rev. Mod. Phys. **55**, 645 (1983).
[13] W. Shockley, Bell Syst. Tech. J. **30**, 990 (1951).
[14] V. Mitin and C. M. Van Vliet, Phys. Rev. B **41**, 5332 (1990).
[15] J. Pozela, in *Hot Electron Diffusion*, edited by J. Pozela (Mokslas, Vilnius, 1981), p. 210.